Int J Clin Exp Med 2021;14(1):37-50
www.ijcem.com /ISSN:1940-5901/IJCEM0120900

Original Article

Research on a three-dimensional finite element model and the stress analysis of thoracolumbar burst fracture in sports training based on modern computer technology

Yaguo Miao[1,2], Jeho Song[2]

[1]Zhengzhou Normal University, Zhengzhou, Henan Province, China; [2]Department of Sports Science, Wonkwang University, Iksan-si, Jeollabuk-do Republic of Korea

Received August 23, 2020; Accepted September 21, 2020; Epub January 15, 2021; Published January 30, 2021

Abstract: Objective: There is high clinical incidence of thoracolumbar burst fracture from sports training, which is mostly caused by axial violence in the thoracic lumbar segments, causing a certain disability rate. Although there are many clinical treatments for thoracolumbar burst fractures, the reports on curative effects are different. At present, the treatment for thoracolumbar burst fractures by posterior short-segment fixation has become a widely accepted surgical method in academic circles. However, because of the loss of support of the anterior column and the middle column caused by the bone defect in the injured vertebral body, there is a high failure rate after posterior short-segment fixation. Methods: Based on modern computer technology, a L1 burst fracture finite element model was established, and the change of internal fixation stress in two periods was studied, in order to provide a biomechanical basis for the treatment of severe thoracolumbar burst fracture by posterior pedicle internal fixation combined with bed rest after. Then, a three-dimensional finite element model of thoracolumbar spine was established using the finite element method, and a stress analysis was carried out to further verify the validity of the model. Finally, the possible mechanism of thoracolumbar spine injury was discussed, which laid a foundation for the next study of the effects of the length of the transfixion screw and the transfixion screw on the biomechanical properties of the spine in an *in vitro* simulation of thoracolumbar fractures. Results: Under vertical compression and compression buckling load, the stress values in the center of the upper and lower endplate of vertebral body and the center of cancellous bone adjacent to endplate were the highest, and there were stress concentration areas in the posterolateral of intervertebral disc annulus, the anterior and posterior parts of thoracolumbar body, the pedicle of compact bone, isthmus and facet joint. Under the load of separation and buckling; the upper edge of spinous process, posterior longitudinal ligament, supraspinous ligament, interspinous ligament and the posterior part of intervertebral disc annulus are all stress concentration sites. Conclusion: The finite element model of this study is in accordance with the clinical characteristics of thoracolumbar osteoporotic vertebral fracture and it well simulates the biomechanical characteristics.

Keywords: Thoracolumbar fracture, sports training, posterior internal fixation, vertebroplasty, three-dimensional finite element

Introduction

The spine is the central axis of the trunk, it is a complex structure composed of many vertebrae connected by intervertebral discs, intervertebral joints and ligaments. The spine forms the spinal canal in the center to accommodate and protect the spinal eruption and cauda equina nerves [1]. The adjacent vertebrae and the intervertebral discs, intervertebral joints and connected ligaments constitute the basic (functional) units of the spine, which bear loads from many different directions and measures, including compression, extension, torsion and shear forces. The intervertebral disc and vertebral body are mainly under pressure, and the annulus fibrosus and the ligaments between the adjacent structures are a under stretching force, while the articular process, annulus fibrosus and the surrounding ligaments are mainly under anti-torsion and shear stresses [2]. On the sagittal plane, the spine forms the physiological lordosis of the cervical spine, the physiological kyphosis of the thoracic spine and the physiological lordosis of the lumbar spine. The thoracolumbar segments (T11-L1) are an anatomical and mechanical transitional region between the physiological lordosis and kyphosis, which is easily damaged, resulting in spinal instability and spinal cord nerve injury [3].

Thoracolumbar burst fracture is a common type of spinal injury found in clinical practice, of which pathological manifestations are often complex and prone to instability of the spinal segments. In addition, the fracture block at the posterior edge of the vertebral body and the intervertebral disc tissue can move backward into the spinal canal to form a space-occupying stenosis in the spinal canal, resulting in spinal cord nerve injury. At present, there is no consensus on how to evaluate the stability of thoracolumbar burst fractures and the influence of the degree of occupation in the spinal canal on spinal nerves. Whether the thoracolumbar fracture needs surgical treatment depends on the stability of the spine and nerve function damage after trauma. In 1949, Nicolltll proposed stable and unstable fractures, indicating that the mechanical stability of the spine is determined by four factors, namely the vertebral body, intervertebral disc, facet joint and interspinous ligament [4]. In 1970, Hold put forward the concept of "column" and posterior ligament complex, where the spine is divided into anterior and posterior columns, and thoracolumbar fractures are classified into two categories according to whether the posterior ligament complex is damaged or not [5]. Aanjabi et al. [6] further studied thoracolumbar fractures and found that the stability of spinal fractures does not depend solely on the integrity of the posterior ligament complex. Denis [7] put forward the theory of three columns of the spine in 1983: the anterior column consists of the anterior longitudinal ligament, the anterior half of the annulus fibrosus and the anterior half of the vertebral body, the middle column consists of the posterior longitudinal ligament, the posterior half of the annulus fibrosus and the posterior half of the vertebral body, and the posterior column consists of the pedicles, interspinous ligaments, supraspinous ligaments, ligaments flavum and facet joints [8].

Thoracolumbar burst fractures are mostly caused by vertical compression and violence. The combined action of buckling and axial stress results in the fracture of the anterior and middle columns of the vertebral body, the fracture of the posterior edge of the vertebral body and the invasion of intervertebral disc tissue into the vertebral canal, resulting in the reduction of the sagittal diameter of the vertebral canal and the stenosis of the vertebral canal [9]. At the same time, kyphosis easily occurs due to the physiological curve of thoracolumbar spine. The treatment for thoracolumbar burst fractures should not only consider any abnormal changes in the local morphology of the fracture, but also accurately evaluate the stability of the fracture and the severity of spinal cord injury. Effective decompression of the spinal canal is an important condition for the recovery of spinal cord nerve function and is also presently one of the principles for treating spinal cord injury [10]. Thoracolumbar burst fractures often lead to spinal stability destruction and spinal cord nerve injury. Abnormal changes in fracture morphology often indicate the possibility of further damage to nerve function and require surgical treatment. However, many studies have found that conservative treatment for thoracolumbar burst fractures without nerve damage results in little or no nerve function damage. Liu et al. [11] analyzed the imaging data and functional evaluation of 136 cases of thoracolumbar burst fractures treated with conservative treatment, and found that conservative treatment is safe and effective for thoracolumbar burst fractures. The shape change, soft tissue (PLC, intervertebral disc), nerve injury of the fracture, and general severity evaluation of thoracolumbar injury should be comprehensively analyzed in the surgical treatment for thoracolumbar burst fracture. TLICS system suggests that surgical treatment should be considered if the comprehensive score is greater than or equal to 5, conservative treatment should be considered if it is less than or equal to 3, and both can be selected if it is 4 [12].

At present, many surgical methods can be used to treat spinal injury, including posterior surgery which uses tension of the posterior longitudinal band for indirect reduction or decompression between posterolateral approaches, and adopts posterior short-segment pedicle screw fixation or long-segment pedicle screw fixation [13]. Due to the need to fix two spinal motions in the normal vertebral body adjacent

Table 1. List of software used in this article

Application software	Full name	Function
MIMICS	Materialise's Interactive Medical Image Control System	Import the scanned CT data in DICOM format. According to CT gray scale, the corresponding organization is distinguished and exported to STL or Cloud point cloud format.
CATIA	Computer-graphics Aided Three-dimensional Interactive Application	Establish a preliminary geometric model, and then carry out denoising, pavement, smoothing and other processing to optimize the geometric structure of the model.
Hypermesh	Hypermesh Software	Grid generation. The cervical vertebra, intervertebral disc, artificial intervertebral disc, intervertebral fusion cage, ligaments and other structural grids are divided.
ANSYS 12.0	Analysis System	Finite Element Modeling and Mechanical Analysis.

to the fractured vertebral body, internal fixation-related complications tend to occur, such as degeneration of adjacent segments, broken nails, broken rods, loosening and pulling out of screws, etc. [14]. Only by carrying out biomechanical finite element simulation of various surgical schemes of finite element internal fixation for lumbar burst fracture, can we create effective evaluation of different surgical schemes with sufficient scientific basis for providing better selection of surgical schemes. Therefore, it is very important to establish various finite element internal fixation models of lumbar burst fracture based on finite element methods for the determination of clinical surgical plan.

In addition, it has been nearly 40 years since Belytschko first reported using the finite element model to study the spine, and the finite element method is widely used in spine surgery and other medical fields as a stress analysis method in engineering science and technology [15]. Currently, with the rapid development of computer information technology, the finite element method can highly simulate the structure of the human body and endow it with biomechanical properties equivalent to the real structure, thus making up for many shortcomings such as a difficulty in obtaining fresh cadaver models, the difference in structure and function between animal models and human beings, and the lack of biological fidelity of physical models in terms of geometry and material properties. In addition, the finite element model also has the advantages of repeatability, accurate data analysis, and simulation of conditions that other methods cannot load or constrain. The role of the finite element method in spine biomechanics will become increasingly obvious. As a new biomechanics research method, it has the ability to randomly change models in order to ascertain the corresponding changes in the internal mechanisms, and it has unique characteristics and advantages, as well as being widely used in various fields of spine therapy. Its research value and advantages are mainly reflected in simulating the pathogenic process of various spinal diseases and exploring the mechanism leading to spinal injury and degeneration [16]. From the perspective of biomechanics, the feasibility of reconstructing spinal stability is revealed, which provides a theoretical basis for the formulation of a spinal surgery plan and the preparation of internal fixation instruments. A great deal of social resources are saved, and the hidden worries in the ethics of entity and cadaver research are eliminated. With the development of digital imaging technology and computer hardware as well as the cross-fusion of achievements in the field of engineering mechanics, the application of the finite element method in the field of spinal internal fixation and bone graft fusion will have a broader prospects [17].

Therefore, based on the concepts of percutaneous vertebroplasty (PVP), a new treatment for spinal injury is proposed in this paper. The key problems include the following aspects: the axial stiffness of T11-L1 segment of the combined PVP screw; whether the average Von-Mises stress of screws and rods exceeds the strength limit; whether the stress of bone tissue around the pedicle screw reaches the strength limit of bone tissue and whether the pull-out strength meets the requirements.

The functional description of the software used in this paper is shown in **Table 1**.

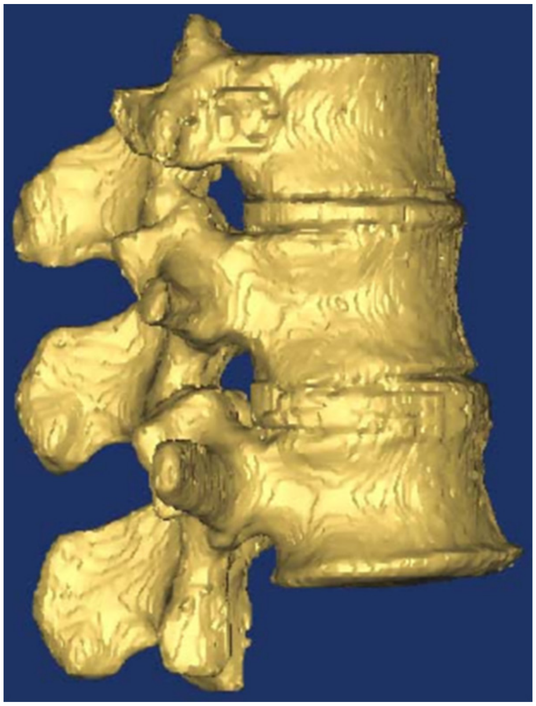

Figure 1. 3D model of T11-L1 vertebral body.

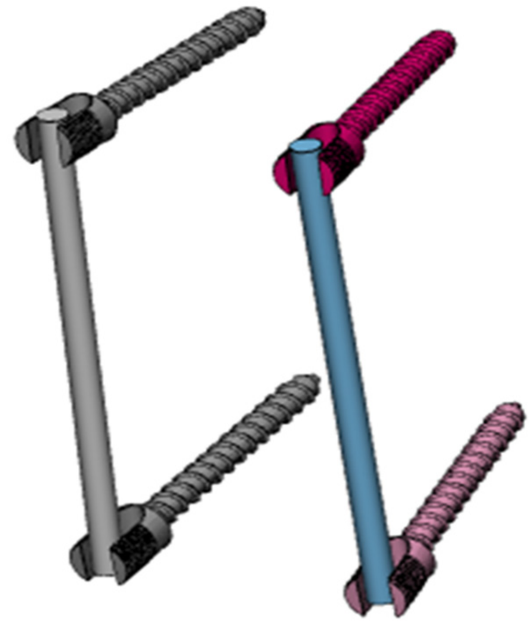

Figure 2. SSPI screw pedicle internal fixation system model.

Materials and methods

Implementation plan

First, a young male volunteer (30 years old) with no history of lumbar trauma or low back pain was selected [18]. Informed consent was obtained from the volunteer. The study protocol was approved by the Ethics Committee of Wonkwang University. After spinal diseases were excluded, his chest and lumbar vertebrae were scanned continuously with 0.625 mm thickness using Discovery CT 750HD spiral CT scanner from GE Company of the United States. The bulb voltage was 120 kV, the bulb current was 268 mA, and the resulting image was stored on a DVD disc in Dicon format and imported into the interactive medical image control system Mimics 10.01.

Then, the DICOM format image was read by Mimics 10.01 software to obtain the T11-L1 image, the threshold of the target image was defined by adjusting the gray value difference between bone tissue and surrounding tissue, the image repair and erasing function were used, and the intervertebral disc tissue was filled with MASK editing function to obtain the T11-L1 vertebral 3D model, as shown in **Figure 1**.

Finally, according to the load sharing score, a L1 severe burst fracture was simulated, a finite element model after posterior pedicle screw fixation was established and 2 months after simulated operation the physiological models were introduced into ANSYS 10.0 software, respectively loaded with 500 N pressure and 15 nm torque to simulate normal physiological flexion and extension and lateral bending of human chest and waist. The deformation and stress distribution of the three models on the vertebral body structure and internal fixation apparatus under different physiological activities were compared [19].

The relevant modeling requirements in this paper are as follows: complete lumbar vertebrae of T11-L1 vertebral bone tissue; T11/L1 intervertebral disc; ligaments anterior longitudinal ligament, posterior longitudinal ligament, joint capsule, ligamentum flavum, interspinous ligament and supraspinous ligament; short segmented pedicle instrumentation (SSPI) and bone cement in injured vertebrae.

Internal fixed geometry reconstruction and global geometry model based on SSPI and PVP

Establishment of pedicle internal fixation system model: In this study, the USS titanium alloy internal fixation system of AO Company was used, and the SSPI internal fixation system

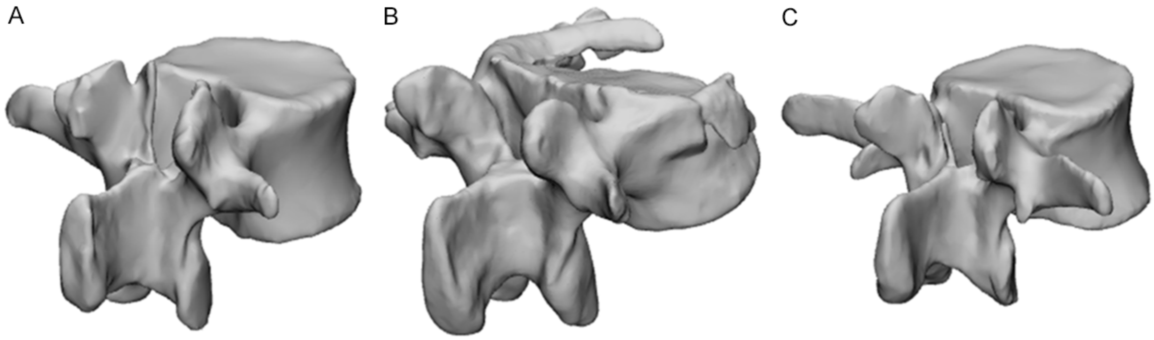

Figure 3. Three-dimensional geometric model of T1~L1 spine. A. T11 spine. B. T12 spine. C. L1 spine.

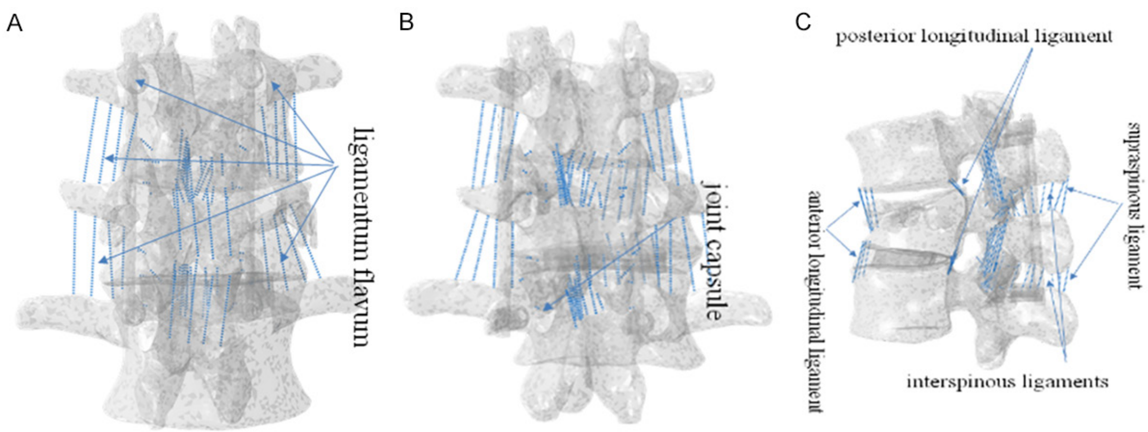

Figure 4. Distribution of ligaments in spine. A. Ligamentum flavum. B. Joint capsule. C. Posterior longitudinal ligament, anterior longitudinal ligament, supraspinous ligament and interspinous ligaments.

model was established in PROE 2.0 software according to the specific parameters such as nail bar. See **Figure 2**.

The pedicle screws in this group were 6.0 mm in diameter, 50.0 mm in length and 6.0 mm in diameter in longitudinal connecting rods, which were stored in *. STL format in preparation for the next simulated fusion and fixation.

Establishment of T11-L1 spine three-dimensional geometric model: The scanned DICOM format file was imported into Mimics software to obtain the thoracolumbar spine image, and the scanned sectional view was displayed from three different perspectives. The threshold of the target image was defined by adjusting the gray scale and contrast of the image, removing soft tissue shadows, selecting the default threshold of the bone system, covering the image shape with editing tools, selecting the desired target area, and running Threshold > Region Growing after the thoracic and lumbar spine mask was selected [20]. The profile of the thoracolumbar spine bone was obtained by repairing and erasing the cross-sectional images with Mimics software internal tools, and the 3D geometric model of the bone was generated by using Cached 3D function as shown in **Figure 3**. Among them, the distribution of spinal ligaments was shown in **Figure 4**.

Establishment of posterior short-segment pedicle internal fixation model: In the established 3D model of T11-L1 vertebral body, with the intersection of the vertical extension line of the outer edge of T11 and L1 superior articular process and the midline of the transverse process as the nail entry point, four pedicle screws were introduced to the ideal position by rotation, translation and other operations, and longitudinal connecting rods were installed to ensure that the screws eid not penetrate the lateral walls of the pedicle and the two sides were balanced and symmetrical by fine tuning, to obtain the posterior short-segment pedicle internal fixation model. See **Figure 5**.

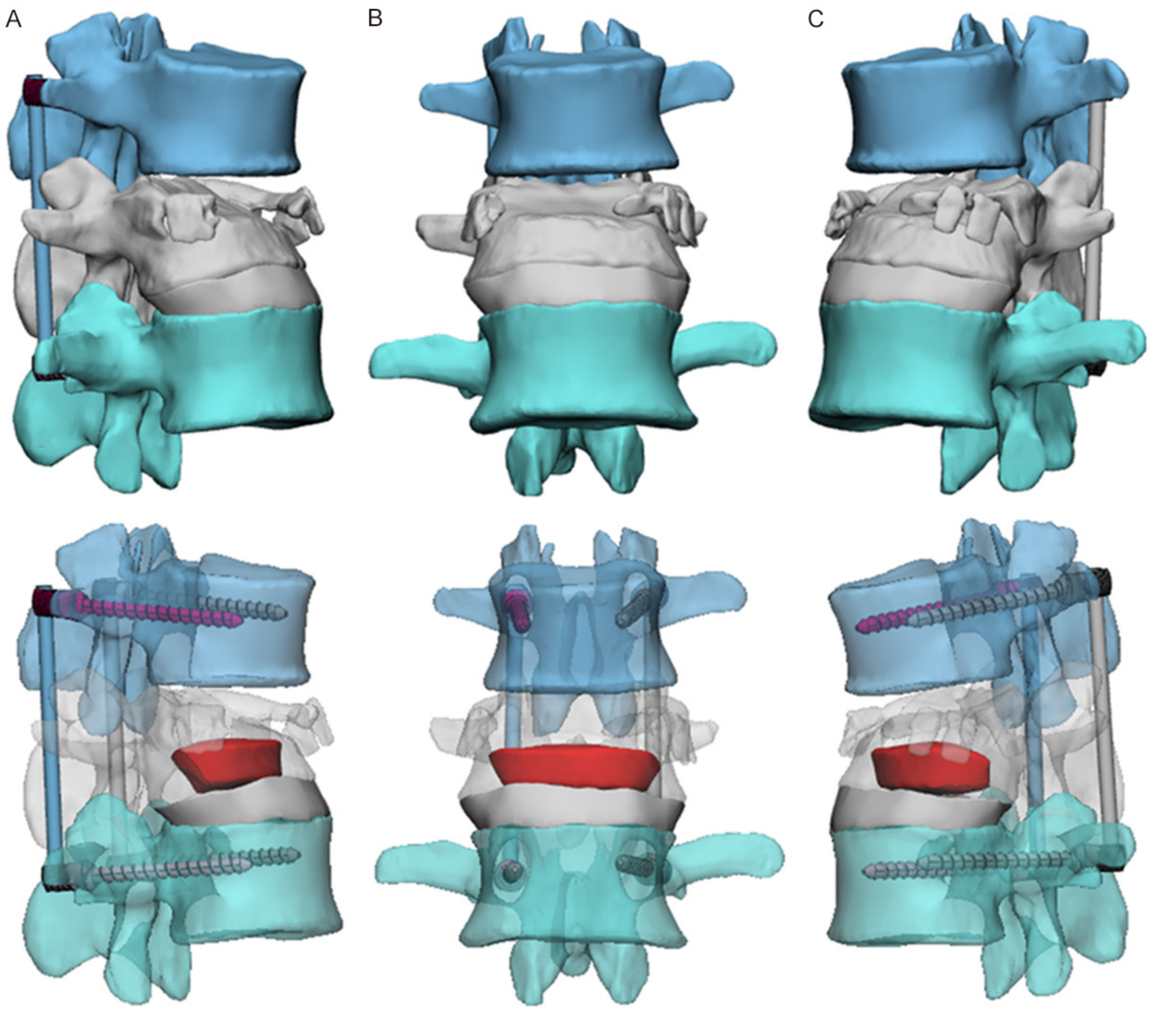

Figure 5. The global geometry model of T11-L1 posterior pedicle internal fixation. A. Left view of geometric model of t11-L1 posterior pedicle screw fixation. B. Front view of the geometric model of t11-L1 posterior pedicle internal fixation. C. Right view of the geometric model of t11-L1 posterior pedicle screw fixation.

Results

Generation of finite element mesh model for internal fixation system based on SSPI and PVP

Establishment of finite element mesh model of pedicle internal fixation system: Based on the three-dimensional geometric model constructed in section 3; firstly, the Hypermesh software Remesh function was used to automatically triangulate the triangular surface mesh, and Stlsmoothner was used to smooth the triangular surface mesh [21]. By increasing the angle parameter value, alternately using Point and Edge reduces the number of triangles. Then, the Reduced with Quality function was selected to reduce the number of wrong triangles, thus obtaining a more accurate triangle model and deleting non-conforming and intersecting triangles [22]. The 3D geometric model was outputed in the format of polygon mesh file .lis for further processing.

Subsequently, the generated thoracic and lumbar spine mesh file was imported into ANSYS 12.0 finite element analysis software and processed according to the following steps: Preprocessor > Element Type > Add > Edit > Delete. Entity unit types were added, real constants and material properties were defined, then Preprocessor > Modeling > Create > Volume > By Area was run, and Pick All to automatically generate thoracolumbar bones was clicked.

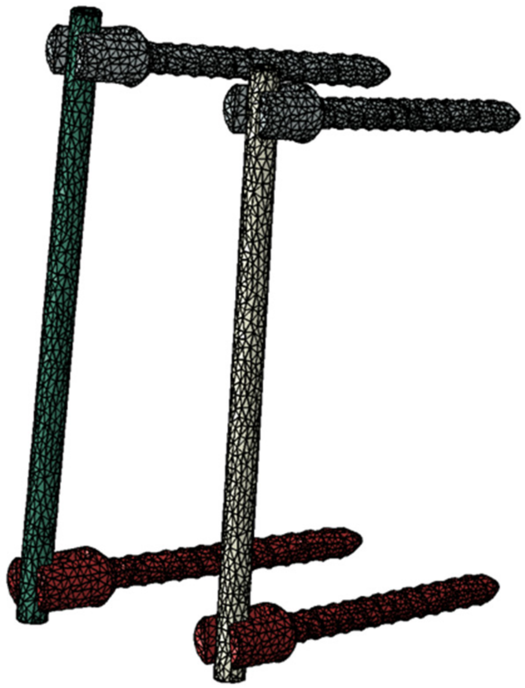

Figure 6. Grid model of SSPI screw pedicle internal fixation system.

Finally, Preprocessor > Messaging > Mesh Tool function to generate the finite element model of bone mesh was selected as shown in **Figure 6**, and the .lis files of element elements and nodes were exported.

Establishment of three-dimensional finite element model of thoracolumbar burst fracture: The thoracic and lumbar spine mesh model generated in MIMICS software was imported into ANSYS 12.0 in .lis format file, and the mesh was optimized again through the steps of surface smoothing and mesh quality inspection. The solid generation function of CFD was used to generate a solid model, that is, to generate a surface triangular shell unit, to form a complete triangular shell to simulate T11-L1 surface cortical bone, to generate a tetrahedral element entity based on the mesh divided on the surface inside, to simulate cancellous bone inside the vertebral body [23], and finally to generate a triangular shell unit with 4290 shells and 242792 tetrahedral elements inside, with a total of 52502 nodes of T11-L1 spine three-dimensional finite element mesh model, as shown in **Figure 7**.

Once the bone model was built, the intervertebral disc and ligament structures were added to the model according to the anatomical position to build a thoracolumbar model conforming to the clinical anatomy, as shown in **Figure 8**.

According to the 3-point criterion of crushing degree in the load sharing score, the elastic modulus of fracture damage was given to 60% of the volume of L1 vertebral body below the upper endplate, and the model of vertebral body nonunion after severe thoracolumbar burst fracture was established. According to the fracture healing model reported by Yang et al. [24], the fractured vertebral body was in the knitting bone formation stage and had a certain strength at 2 months after operation. The elastic modulus was given to the cortical bone in 60% of the vertebral body below the upper endplate, while the elastic modulus of the fibrous tissue was given to the original cancellous bone, and thus a model of healing 2 months after the severe thoracolumbar burst fracture was established.

This experimental model includes T11-L1 vertebral bodies and 3 intervertebral discs, which were composed of cancellous bone and cortical bone, and were simplified into continuous uniform and same-sex linear elastic materials by tetrahedron simulation. The intervertebral disc was simulated by the shell and core, the intervertebral disc and the endplate were defined as face-to-face contact, and the ligaments were simulated by non-linear materials. The motion between the articular surfaces was complicated, and when the gap was too large or too small, interaction will occur in multiple directions. For this reason, the articular surfaces as point-to-point contact units were defined.

Finally, the cortical bone, cancellous bone, posterior structure, intervertebral disc, ligaments, internal fixation materials, are routinely assigned (as shown in **Tables 2**-**4**). The connection between each facet joint was treated as two frictionless contact surfaces.

Stress analysis of 3D finite element model based on SSPI and PVP

Boundary conditions and loading: Through the stress cloud picture under the dynamic impact test (**Figure 9**), it was found that the stress was mainly concentrated in the front edge of the vertebral body and transmitted down the cortical bone, the vertebral arch root and its surrounding cortical bone were also the stress

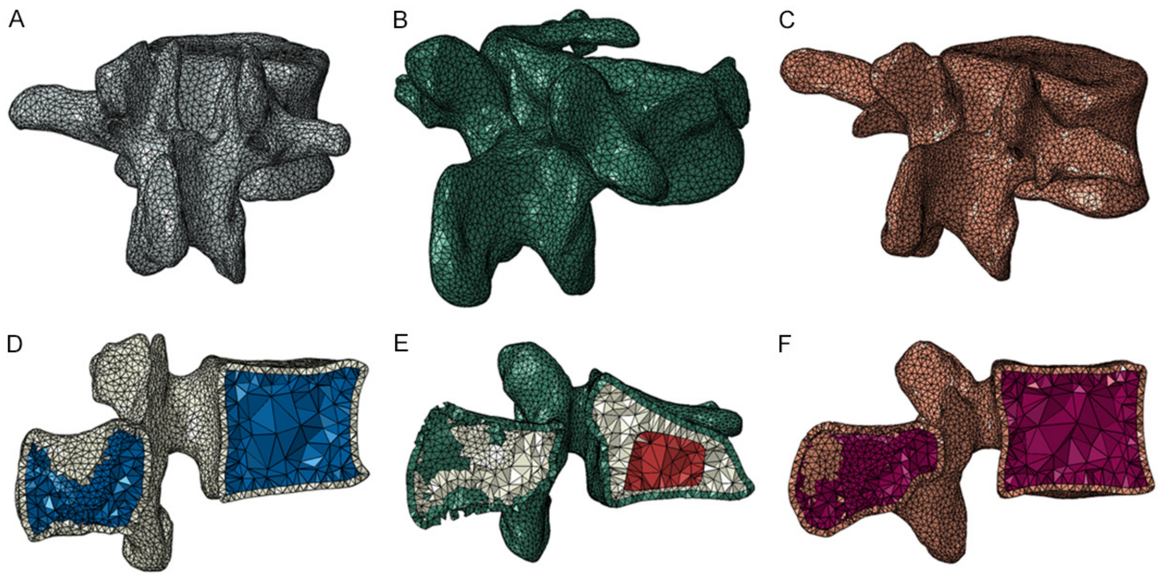

Figure 7. Three-dimensional finite element mesh model of T11~L1 spine. A. T11 spine. B. T12 spine. C. L1 spine. D. T11 fracture surface. E. T12 fracture surface. F. L1 fracture surface.

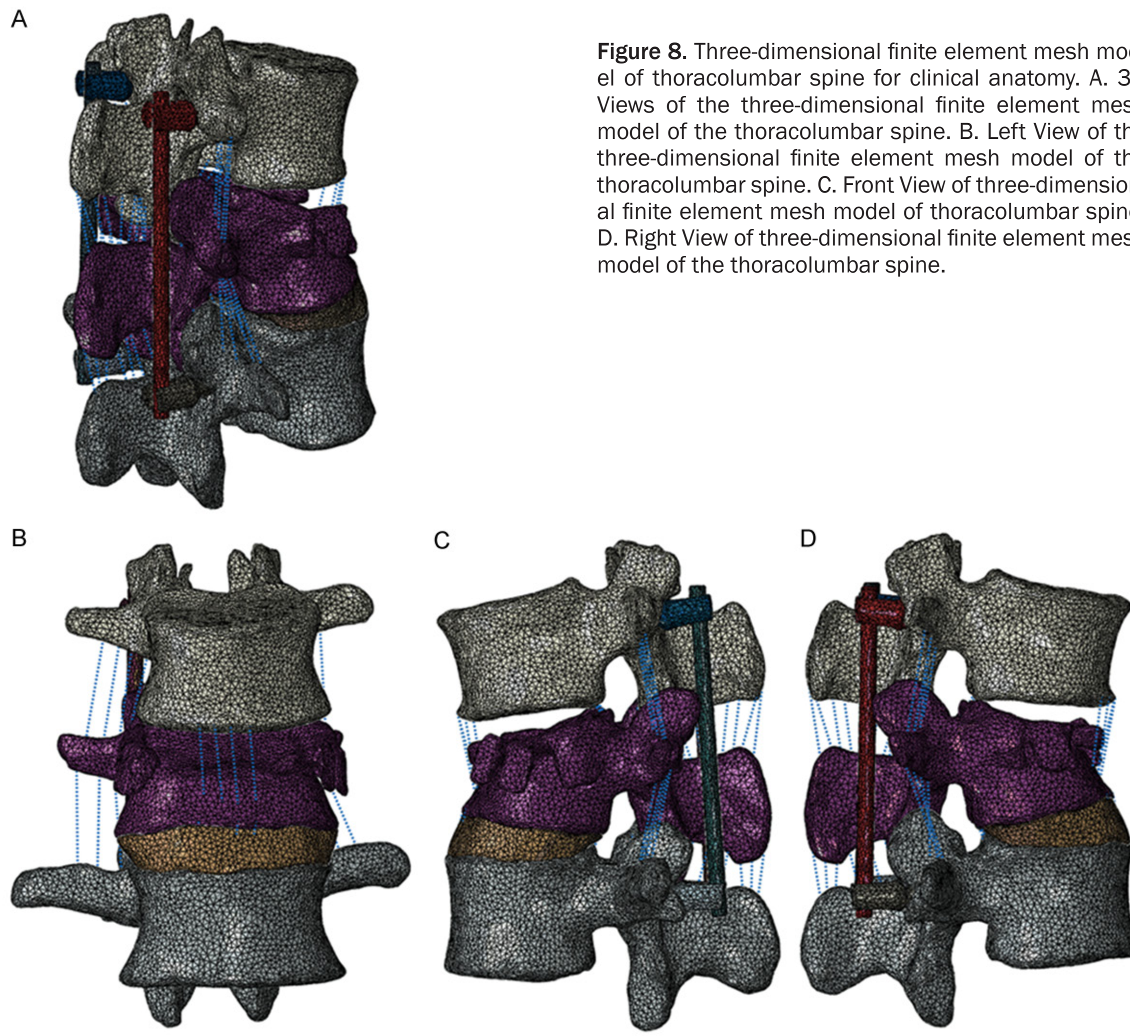

Figure 8. Three-dimensional finite element mesh model of thoracolumbar spine for clinical anatomy. A. 3D Views of the three-dimensional finite element mesh model of the thoracolumbar spine. B. Left View of the three-dimensional finite element mesh model of the thoracolumbar spine. C. Front View of three-dimensional finite element mesh model of thoracolumbar spine. D. Right View of three-dimensional finite element mesh model of the thoracolumbar spine.

Table 2. Properties of structural materials in various parts of spine

Attribute		Modulus of Elasticity (Mpa)	Poisson's Ratio
Vertebral Body	Cortical Bone	12000	0.29
	Cancellous Bone	200	0.29
Intervertebral Disc	Nucleus Pulposus	4.2	0.45
	Fiber Ring	1.	0.49

Table 3. Material properties of internal fixtures

Bone	Unit	Node	Unit type
L1	11735	3741	Tetrahedron
L3	13178	4157	Tetrahedron
L4	22465	6277	Tetrahedron
L5	22191	6300	Tetrahedron
S1-3	52540	14378	Tetrahedron
Fiber Ring	2556	851	Tetrahedron
Nucleus Pulposus	2755	910	Tetrahedron
Ligament	112	224	Rod unit
Left Titanium Plate	37729	10149	Tetrahedron
Right Titanium Plate	36826	10031	Tetrahedron
Screw	5078	1682	Tetrahedron

concentration areas, and the stress was the largest at the junction between the outer lower edge of the pedicle and the vertebral body, spreading to the vertebral body along this point, while the stress of cancellous bone was significantly less than that of cortical bone.

Ignoring the fretting between the lumbar screws and the bone, the pedicle screws and the screw channel were defined as tight connection without sliding and compression deformation (**Figure 10**). Constrained boundary: Without any constraint, it receives the load of simulation and part weight in the center of the upper edge of the vertebral body, while the degree of freedom in all directions of all nodes of the lower edge of the vertebral body was limited [25]. The assumption was that the material properties of biological materials involved in this finite element analysis were assumed to be homogeneous, continuous and isotropic. When receiving the load, the elements of the model maintain sufficient stability, and there is no mutual sliding between the sections, regardless of the stress and deformation of each part of the material in the process of receiving the load. Loading conditions: The average weight of the simulated head applied above is preloaded, and the additional pure moment of motion is added. According to the above constraints and loading conditions, the relevant data are imported into the finite element software for finite element analysis.

The loading situation is as follows: (1) forward-buckling and backward - stretching loading: adding 15 N.m X-axis bending moment to the axial loading of 500 N; (2) lateral buckling load: adding 15 N.m Y-axis bending moment on the basis of 500 N axial load; (3) rotational loading: on the basis of 500 N axial loading, 15 N.m Z-axis bending moment is added.

SSPI and PVP internal fixation vertebral displacement: The maximum displacement data of physiological, post-operative and post-operative 2-month models under simulated human body flexion, extension and lateral bending loads were recorded (**Table 5**). The smaller the displacement, the greater the stiffness and the better the stability of the vertebral body after internal fixation. In the three states, the maximum displacement was 2.574 mm in the flexion state of the postoperative model, while the displacement of the postoperative model in the flexion state and lateral bending state was larger than that of the other two groups, indicating that the stability of the postoperative model was worse than that of the other two groups. The maximum displacement of the model after surgery was 168%, 52% and 150% of that of the physiological model under flexion, extension and lateral bending respectively. The maximum displacement of the model after surgery was 101%, 51% and 92% of that of the physiological model under the three working conditions of the 2-month model after surgery. The stability of the model after giving certain strength to the anterior and middle columns of the vertebral body has basically reached normal physiological state.

In this study, the displacement and stress distribution of physiological model, fracture model after operation and fracture model 2 months after operation were compared under the three working conditions of flexion, extension and lat-

Table 4. Ligament property

Ligament Position	Elastic Modulus (Mpa)	Poisson's Ratio	Area of Section (mm^2)
Anterior Longitudinal Ligament	30.0	0.40	6.1
Posterior Longitudinal Ligament	20.0	0.40	5.4
Ligamentum Flavum	10.0	0.40	50.1
Sup rachial Ligament	1.5	0.40	13.1
Interspinous Ligament	10.0	0.40	13.1
Joint Capsule Ligament	10.0	0.40	46.6

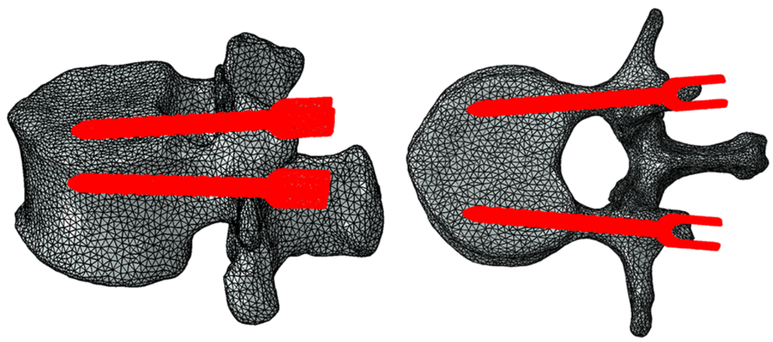

Figure 9. Pedicle screw implantation in vertebral body.

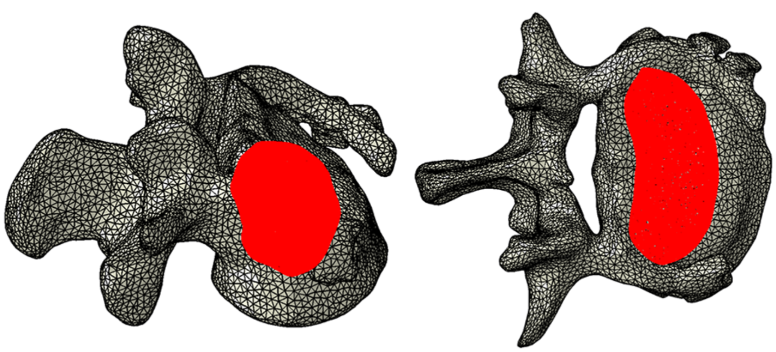

Figure 10. Cement filling diagram.

Table 5. Maximum displacement (mm) of pedicle internal fixation system in three states

Part	Physiological Model	Postoperative Model	2-Month Model After Operation
Proneness	1.534	2.574	1.553
Extension	0.299	0.153	0.151
Lateral Flexion	0.842	1.264	0.776

eral flexion (**Figure 11**). Under the anterior flexion condition, the maximum displacement (mm) of the physiological model, the fracture model after operation and 2 months after operation were 1.534, 2.574 and 1.553 respectively, located in front of the vertebral body. Compared with the physiological model, after simulating severe burst fracture injury, the displacement of the vertebral pedicle internal fixation system (67.8%) was still larger than the physiological situation, indicating that the stiffness of the vertebral body was obviously decreased after the anterior and middle columns of the vertebral body were crushed, and the posterior internal fixation could not maintain the physiological stiffness when the spinal column was flexed. This result supported Mc-Cormack's conclusion that severe thoracolumbar burst fractures should be treated by anterior surgery, because previous studies recognized that anterior surgery was stiffer than physiological conditions under flexion. When the cortical bone in the anterior and middle columns of the vertebral body healed to a certain strength 2 months after operation, the displacement of the posterior pedicle internal fixation system under the anterior flexion condition was very close to the physiological condition, indicating that the spinal stiffness can be restored to the physiological level 2 months after the posterior pedicle internal fixation, which provides a theoretical basis for the clinical posterior operation for the treatment of severe thoracolumbar burst fractures. The pedicle internal fixation system enhances the stability of the posterior column of the spine, so the displacement of the model after operation and 2 months after operation was smaller than that of the physiological model, and the displace-

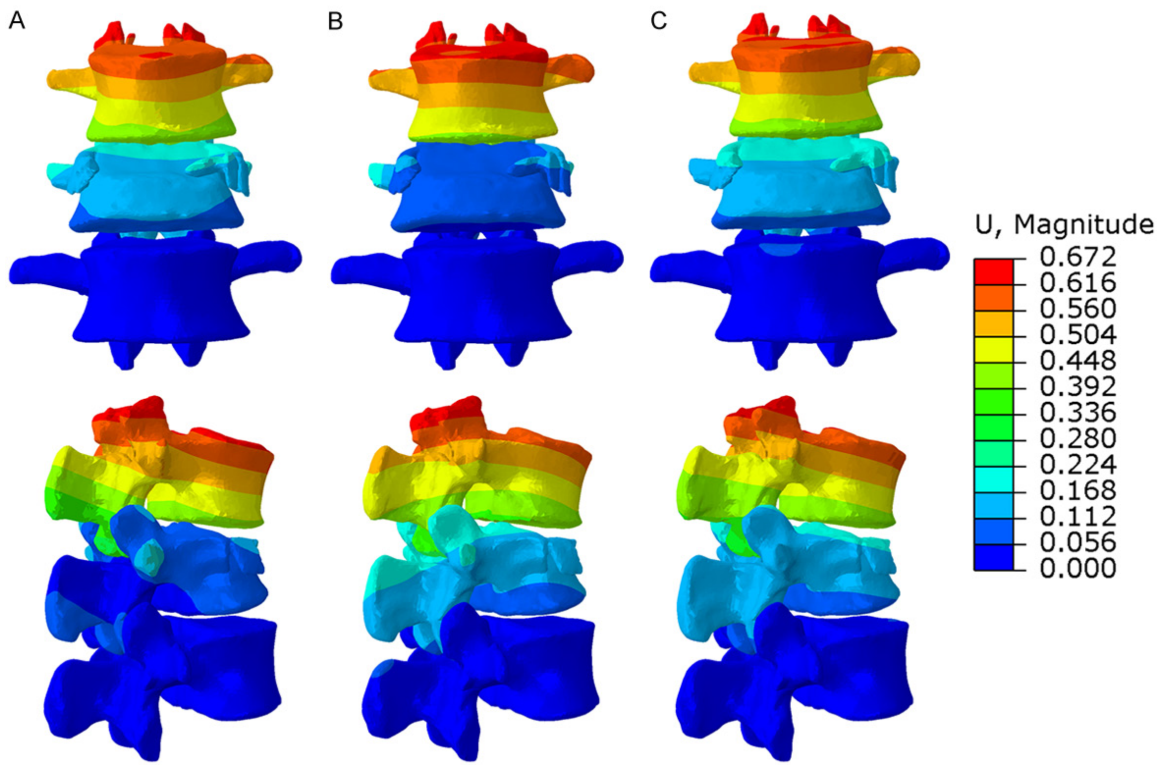

Figure 11. Displacement map of postoperative model in three states. A. Displacement diagram of anteflexion state. B. Displacement diagram of rear protraction state. C. Displacement diagram of lateroflexion state.

Table 6. Maximum stress value (mpa) of pedicle internal fixation system in three states

Part	Postoperative model	2-month model after operation
Proneness	474.919	286.421
Extension	86.119	82.259
Lateral Flexion	262.864	179.188

ment between the model after operation and 2 months after operation was almost the same, proving that the stiffness of the posterior column of the spine after operation was mainly borne by the internal fixation. In the simulation of lateral bending, the maximum displacement of the three models were all located at the front edge of one vertebral body, and the results were similar to those of anterior flexion. The displacement of the postoperative model was 50.2%, greater than that of the physiological model, indicating that the stiffness provided by posterior pedicle internal fixation could not meet the immediate anterior flexion or lateral bending. The displacement of the model in the second month after surgery was close to that of the physiological model, which was related to the strength of the anterior column and the partial support provided by the posterior internal fixation during lateral bending.

Stress State of SSPI and PVP internal fixation vertebral body: The maximum stress of the internal fixation system was recorded after operation and 2 months after operation under the load of simulating human body flexion, extension and lateral bending (**Table 6**). From the stress distribution diagram (**Figure 12**), it can be seen that the stress concentration of the internal fixation system under various working conditions was at the root of the pedicle screw, which was consistent with the common fracture site of internal fixation in clinic.

Discussion

Under the three working conditions, the maximum stress of internal fixation is 474.919 MPa in the pre-flexion state and the lack of support in the anterior and middle columns of the model vertebral body after operation. In contrast, the maximum stress of the internal fixation system was 286.421 MPa at 2 months after oper-

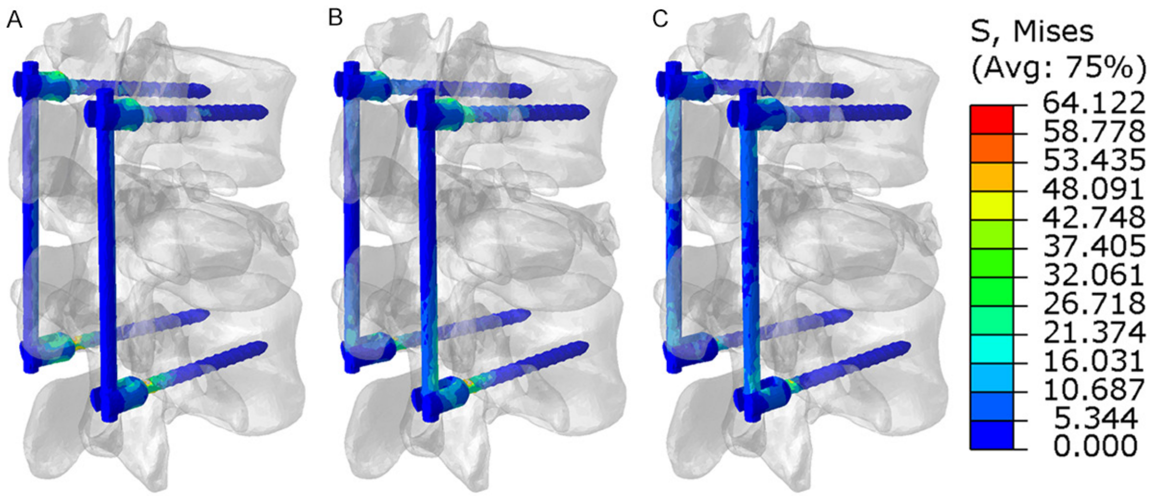

Figure 12. Stress distribution diagram of internal fixation system in three states of postoperative model. A. Stress distribution diagram of the internal fixation system in Anteflexion state. B. Stress distribution diagram of the internal fixation system in Rear Protraction state. C. Stress distribution diagram of the internal fixation system in Lateroflexion state.

ation, when the anterior and middle columns had healed to a certain extent. In the lateral bending state, the results of the two groups were similar to those of the forward bending. In the extended state, the stress was mostly concentrated on the internal fixation system and the posterior structure of the vertebral body, and the damaged anterior and middle columns have relatively little influence on the results, so the stress results between the two groups were similar.

The stiffness of the physiological model under vertical pressure was within the range of previous *in vitro* measured results and has passed the validity test. From the point of view of displacement distribution, the maximum displacement of the model after surgery was 168%, 52% and 150% of that of the physiological model under flexion, extension and lateral bending, respectively. The maximum displacement of the model after surgery was 101%, 51% and 92% of that of the physiological model under three working conditions. The model after surgery was closer to normal physiological state under flexion and lateral bending, and more stable than the physiological model under extension. According to the distribution of internal fixation stress, the internal fixation stress was concentrated at the root of pedicle screw under three working conditions. The maximum stress values of the model 2 months after operation were 60%, 99% and 68% of that of the model in the cases of flexion, extension and lateral bending, respectively. The stress borne by the internal fixation 2 months after operation was less than that of the model after operation.

At present, when the finite element method is used to study thoracolumbar burst fractures, the L1 vertebral body is usually partially excised on the normal physiological T11-L1 segment or the elastic modulus of bone damage is input to the L1 vertebral body, and thus the thoracolumbar burst fracture model is simulated. The purpose of this study was to verify the feasibility of posterior pedicle screw fixation system in the treatment of severe thoracolumbar burst fractures with a load sharing score of 7-9. Therefore, this study hopes to improve the original fracture model according to McCormack's load sharing scoring system and make it more in line with the purpose of this study. The load-sharing scoring system is divided into three aspects: the degree of fragmentation of the vertebral body, the degree of displacement of the fractured vertebral body, and the degree of correction of kyphosis, with a score of 1-3 points for each aspect. The higher the combined score of the three points, the more serious the fracture is. Among them, the score of vertebral crushing degree exceeded 60%.

In this study, 60% of the volume below the upper endplate of the L1 vertebral body was given the elastic modulus of bone injury. However, clinical practice has proved that posterior pedicle internal fixation system can effectively correct kyphosis and reduce vertebral fracture to a normal level. Therefore, the placement of internal fixation system in the upper and lower segments of the “injured vertebral body” conforms to the clinical practice. This study simulated two fracture models after internal fixation and 2 months after operation by changing the elastic modulus of L1 bone injury. After pedicle internal fixation of thoracolumbar fractures, the originally crushed and compressed vertebral body was restored to normal state, but the anterior and middle columns were in a “hollow” state after reduction, with extremely low mechanical strength. Therefore, the elastic modulus of this part of the vertebral body (including cortical bone and cancellous bone) was assigned to 1 MPa in this study, which was negligible compared with the elastic modulus of the normal vertebral body. At the restoration of fractured vertebral body was at the knitting bone formation stage and had a certain strength 2 months after operation. CT reconstruction revealed that the inside of the injured vertebral body showed “eggshell-like” changes, but the surrounding bone cortex showed signs of callus healing. Therefore, we assign the original cancellous bone inside the L1 vertebral body to the elastic model of fibrous tissue, and the cortical bone in the original “bone injury” part to the elastic modulus at the callus stage according to Yang’s description of the elastic modulus at the second month of vertebral fracture healing [24].

Conclusion

In this paper, a three-dimensional finite element model of the normal T11-L1 segment was built, and the biomechanical finite element simulation of various finite element internal fixation schemes for lumbar burst fracture was further carried out, based on which different surgical schemes were evaluated effectively to provide sufficient scientific basis for selecting surgical schemes. Firstly, the implementation plan and physiological models of T11-L1 vertebral body were given, as well as the related analysis software used in this study. Secondly, the whole geometric model of pedicle internal fixation system based on SSPI and PVP and the three-dimensional geometric model of T11-L1 spine were constructed; thus the short-segment pedicle internal fixation model of T11-L1 spine posterior can be obtained. Thirdly, the finite element mesh model of the relevant internal fixation system and the three-dimensional finite element mesh model of thoracolumbar spine suitable for clinical anatomy were obtained, and the material properties and ligament properties used in this study were also presented. Finally, under the torque of 15 N/m, the validity of the three-dimensional finite element model of the mobility of T11, T12 and L1 vertebral bodies were verified, and the stress state of the model after operation were analyzed. According to the load sharing score, the finite element model of L1 severe burst fracture after pedicle screw fixation and 2 months later were simulated, proving that the stability of the model 2 months after operation was better than that of the model after operation in the load loading experiment, which was similar to the physiological situation. The method of treating severe thoracolumbar burst fracture with posterior pedicle internal fixation system studied in this paper provides theoretical basis for clinical application, and can achieve good biomechanical performance combined with bed rest after operation.

Disclosure of conflict of interest

None.

Address correspondence to: Jeho Song, Department of Sports Science, Wonkwang University, Iksan-si, Jeollabuk-do Republic of Korea. Tel: +82-63-850-6895; E-mail: jehosong95@163.com

References

[1] Liao JC, Fan KF, Keorochana G, Chen WJ and Chen LH. Transpedicular grafting after short-segment pedicle instrumentation for thoracolumbar burst fracture: calcium sulfate cement versus autogenous iliac bone graft. Spine (Phila Pa 1976) 2010; 35: 1482-1488.

[2] Eleraky MA, Duong HT, Esp E and Kim KD. Expandable versus nonexpandable cages for thoracolumbar burst fracture. World Neurosurg 2011; 75: 149-154.

[3] Shi R, Liu H, Zhao X, Liu X, Gong Q, Li T, Liu L, Zeng J and Song Y. Anterior single segmental decompression and fixation for Denis B type thoracolumbar burst fracture with neurological deficiency: thirty-four cases with average twenty-six month follow-up. Spine (Phila Pa 1976) 2011; 36: E598-605.

[4] Xu JG, Zeng BF, Zhou W, Kong WQ, Fu YS, Zhao BZ, Zhang T and Lian XF. Anterior Z-plate and titanic mesh fixation for acute burst thoracolumbar fracture. Spine (Phila Pa 1976) 2011; 36: E498-504.

[5] Ökten A, Gezercan Y, Özsoy KM, Ateş T, Menekşe G, Aslan A, Çetinalp E and Güzel A. Results of treatment of unstable thoracolumbar burst fractures using pedicle instrumentation with and without fracture-level screws. Acta Neurochir (Wien) 2015; 157: 831-836.

[6] Alizadeh M, Kadir MR, Fadhli MM, Fallahiarezoodar A, Azmi B, Murali MR and Kamarul T. The use of X-shaped cross-link in posterior spinal constructs improves stability in thoracolumbar burst fracture: a finite element analysis. J Orthop Res 2013; 31: 1447-1454.

[7] Zhao X, Fang XQ, Zhao FD and Fan SW. Traumatic canal stenosis should not be an indication for surgical decompression in thoracolumbar burst fracture. Med Hypotheses 2010; 75: 550-552.

[8] Moon YJ and Lee KB. Relationship between clinical outcomes and spontaneous canal remodeling in thoracolumbar burst fracture. World Neurosurg 2016; 89: 58-64.

[9] Deqing L, Kejian L, Teng L, Weitao Z and Dasheng L. Does the fracture fragment at the anterior column in thoracolumbar burst fractures get enough attention? Medicine (Baltimore) 2017; 96: e5936.

[10] Özbek Z, Özkara E, Önner H, BaŞ G, Erman İC, Özen H, Entok E and Arslantaş A. Treatment of unstable thoracolumbar fractures: does fracture-level fixation accelerate the bone healing? World Neurosurg 2017; 107: 362-370.

[11] Liu JY and Liu SZ. Vertebra 3 nailing 5 and fracture vertebral bony graft in the treatment of thoracolumbar burst fracture. Clin Med 2012.

[12] Wang Z and Wang R. Treatment of thoracolumbar burst fracture with posterior open reduction internal fixation. Clin Med 2010.

[13] Hao D, Wang W, Duan K, Ma M, Jiang Y, Liu T and He B. Two-year follow-up evaluation of surgical treatment for thoracolumbar fracture-dislocation. Spine (Phila Pa 1976) 2014; 39: E1284-1290.

[14] Pan T, Qian BP and Qiu Y. Comparison of sagittal spinopelvic alignment in patients with ankylosing spondylitis and thoracolumbar fracture. Medicine (Baltimore) 2016; 95: e2585.

[15] Chen J, Xie CL, Xuan J, Yan YZ, Dou HC, Zheng ZM, Chen Y, Chen XB, Wang XY and Wu AM. A novel knotless barbed suture technique for traumatic thoracolumbar fracture in posterior surgery. World Neurosurg 2018; 114: e1031-e1037.

[16] Mohamadi A, Googanian A, Ahmadi A and Kamali A. Comparison of surgical or nonsurgical treatment outcomes in patients with thoracolumbar fracture with Score 4 of TLICS: a randomized, single-blind, and single-central clinical trial. Medicine (Baltimore) 2018; 97: e9842.

[17] Li S, Li Z, Hua W, Wang K, Li S, Zhang Y, Ye Z, Shao Z, Wu X and Yang C. Clinical outcome and surgical strategies for late post-traumatic kyphosis after failed thoracolumbar fracture operation: case report and literature review. Medicine (Baltimore) 2017; 96: e8770.

[18] Xu S, Zhang XW and Na Q. Application of median pedicle screw technique in the single segmental thoracolumbar fracture. Clin Med 2016.

[19] Boakye M, Arrigo RT, Hayden Gephart MG, Zygourakis CC and Lad S. Retrospective, propensity score-matched cohort study examining timing of fracture fixation for traumatic thoracolumbar fractures. J Neurotrauma 2012; 29: 2220-2225.

[20] Zhao Q, Zhang H, Hao D, Guo H, Wang B and He B. Complications of percutaneous pedicle screw fixation in treating thoracolumbar and lumbar fracture. Medicine (Baltimore) 2018; 97: e11560.

[21] Liu P, Li YA and Zhao JH. Selective surgical treatment of burst fractures of thoracolumbar junction via posterior short-segment fixation and fusion. J Traumatic Surg 2008.

[22] Zhao D, Chen YB, Chen SL and Luo SW. Effects of alendronate sodium tablet in prevention of refracture after osteoporotic thoracolumbar vertebral compression fracture in 80 cases. China Pharmaceuticals 2017.

[23] Dodd CA, Fergusson CM, Pearcy MJ and Houghton GR. Vertebral motion measured using biplanar radiography before and after Harrington rod removal for unstable thoracolumbar fractures of the spine. Spine (Phila Pa 1976) 1986; 11: 452-455.

[24] Yang YU, Fan HQ and Chen M. Comparison of consecutive pedicle screw fixation and short-segment pedicle screw fixation in treatment of thoracolumbar fracture. J Spinal Surg 2012.

[25] Qiu YX, Zhang SQ, Jin XB, Xiao QS and Zeng B. Study on clinical efficacy of vertebroplasty and pedicle screws in the treatment of thoracolumbar vertebral compression fractures. Xiandai Shengwuyixue Jinzhan 2015.